Classical Scaling of the Quantum Capacitances for Molecular Wires

James C. Ellenbogen,* Carl A. Picconatto, and Jacob S. Burnim
Nanosystems Group, The MITRE Corporation, McLean, Virginia 22102, USA

(Dated: April 2, 2007)

Detailed calculations demonstrate that the quantum capacitances of non-spherical, rod-like molecular wires scale with their dimensions according to a linear law much like that obeyed by classical, macroscopic spherical capacitors. Further, this linear "isoperimetric" scaling law leads to a particularly simple formula that relates a molecule's electron affinity directly to its ionization potential and its spatial dimensions.

I. INTRODUCTION

A fundamental problem of atomic and molecular quantum mechanics is to determine the excitation energies and electron detachment energies of atoms and molecules from the nuclear charges and the dimensions of the systems. In the conventional quantum approach to this problem, the relationship between the dimensions and the energies is expressed indirectly through the complex, computationally intensive solution of many-electron, integro-differential quantum wave equations. However, the results of such calculations, as described elsewhere for atoms [1] and as described here for molecules, suggest that there might be an alternate, simpler, direct approach to connecting the dimensions of quantum systems and their energetics. This approach takes advantage of the principles of electrostatics and a developing body of evidence that atoms and molecules behave much like macroscopic spherical capacitors, with their shapes and their dimensions controlling their energies through their capacitances.

Specifically, it is demonstrated in this paper that the quantum capacitances of non-spherical, rod-like molecular wires vary or "scale" according to a linear law much like that obeyed by classical spherical capacitors. Further, this linear isoperimetric [2] scaling law for the capacitances leads to a simple formula that relates a molecule's difficult-to-calculate electron affinity (EA) directly to its ionization potential (IP) and its spatial dimensions.

To those ends, we describe a detailed computational exploration of the scaling of the quantum capacitances with molecular dimensions for oligomeric polyphenylene ethynylene (OPE) molecules. (See Fig. 1.) The results of extensive density functional theory (DFT) calculations, as presented in Fig. 2 and Table I, initially reveal that the quantum capacitances [3–5] of the OPE molecular wires scale as a logarithm of the molecules' lengths.

However, as is also shown in Fig. 2, this unusual logarithmic capacitance scaling behavior, which required thousands of hours of complex quantum mechanical computer calculations to determine, can be reproduced to an excellent approximation by a very simple formula from the theory of isoperimetric inequalities [2] in classical electrostatics:

$$C = 4\pi\epsilon_0\kappa(abc)^{\frac{1}{3}} + C_0. \qquad (1)$$

Parameters a, b, and c are the semiaxial dimensions of an ellipsoid that models the approximately ellipsoidal mean contour of the electron distribution for the π-type highest occupied molecular orbital (HOMO) of an OPE molecule.

In isoperimetric theory [2], the first term on the right of Eq. (1) evaluates the classical capacitance of an isolated spherical conductor with a volume equivalent to that of the ellipsoidal HOMO or valence shell. Then, if we define the isoperimetric "equivalent radius" of that sphere as $r_{eq} = (abc)^{\frac{1}{3}}$, it follows that the OPE quantum capacitances C_I that are approximated by C from Eq. (1) should be linear in r_{eq} or nearly so. This is seen in Fig. 3.

The linear scaling of the capacitance with r_{eq} also can explain mathematically the logarithmic form of the scaling with L. This is shown below in Section III.

Within Eq. (1), the slope of the scaling line in r_{eq} is written as $4\pi\epsilon_0\kappa$ to emphasize the similarity of this linear
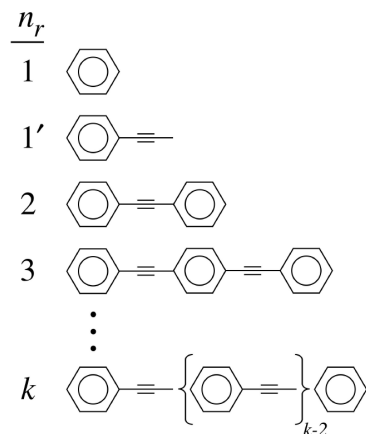

FIG. 1: Structures for a sequence of oligomeric polyphenylene-ethynylene (OPE) molecular wires of increasing ring numbers n_r and lengths L.
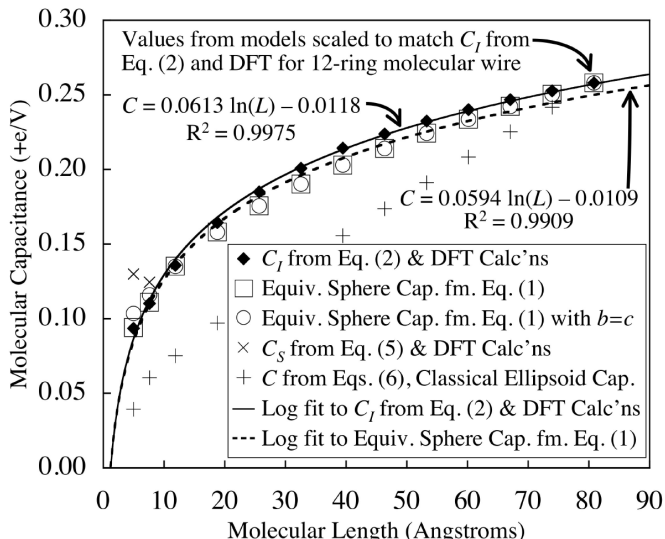
*Electronic address: ellenbgn@mitre.org

FIG. 2: Capacitances C_I (black diamonds) and C_S (×'s) of molecular wires from detailed quantum calculations are plotted vs. the molecules' lengths, along with scaled capacitances (circles, squares, and pluses) from three quasi-classical ellipsoidal models. Values plotted are given in Table I. Points for C_S are omitted for $n_r \geq 2$, because $C_S = C_I$ in those cases. Squares represent a model based upon a sphere, with its volume equivalent to that of a 3-axis ellipsoid having the approximate mean dimensions of the HOMO. This reproduces the unusual logarithmic scaling behavior of the quantum capacitances (black diamonds).
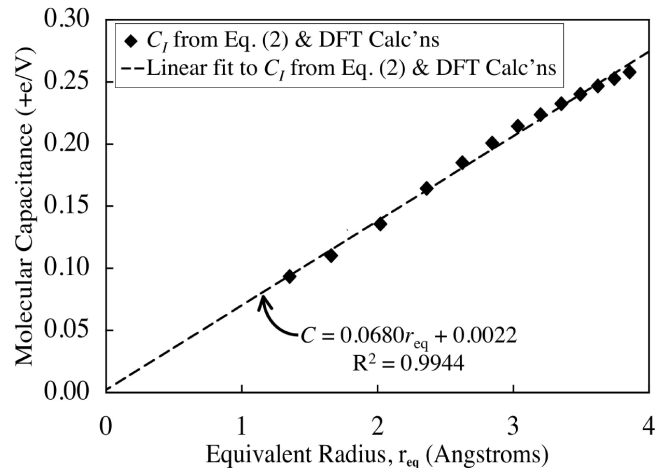

FIG. 3: Capacitances C_I (black diamonds) from detailed quantum calculations are plotted vs. the equivalent radii, $r_{eq} = (abc)^{1/3}$, of the molecules, where a, b, and c are the semiaxes of the molecules' approximately ellipsoidal valence electron distributions. As seen from the regression line (dashes), C_I is an approximately linear function of r_{eq}, with $\kappa = \text{slope}/(4\pi\epsilon_0) = 0.979$ from Eq. (1) and the slope of the line.

capacitance scaling relation for a non-spherical molecule to the one in classical electrostatics for a sphere [6] with radius r_{eq}. The scaling parameter κ may be interpreted as a dielectric constant for the $(N-1)$-electron medium surrounding an N-electron system's valence shell [1] and has the same value for all the OPE molecules. Constant ϵ_0 is the permittivity of free space.

The term C_0 is the intercept of the scaling line in r_{eq} with the vertical, capacitance axis. This non-zero intercept has no analog in a scaling relation for an isolated classical conductor. However, for the quantum capacitances of these molecules, as in the case of atoms [1], the nonzero intercept may be understood as an effect of capacitive coupling of the highest occupied orbital to the lowest unoccupied orbital, which acts like a "virtual" outer conductor, even for an isolated molecule or atom.

The demonstration below of Eq. (1) for the capacitances of OPE molecules is a step by the authors toward generalizing to neutral molecules a linear, quasi-classical capacitance scaling relation that recently was demonstrated [1] for neutral atoms. The linear relation that applies to the atoms is similar in form to Eq. (1), excepting that for atoms r_{eq} is supplanted by $\langle r \rangle_a$, the mean radius of the highest occupied atomic orbital.

II. METHOD AND RESULTS

Figure 1 depicts the structures of a series of OPE molecules with increasing numbers of rings n_r and lengths L, while Table I summarizes the results of our DFT calculations of their structures, IPs, EAs, and capacitances. Following Iafrate et al. [3], as well as Gazquez and Ortiz [4] and Perdew [5], the capacitance of an atom or molecule may be evaluated

$$C_I = 1/(I - A). \tag{2}$$

Perdew [5] emphasized the scale independence of this equation, which evaluates the capacitance for an N-electron quantum system with total energy $E(N)$, having a first IP

$$I = E(N - 1) - E(N) \tag{3}$$

and an EA

$$A = E(N) - E(N + 1). \tag{4}$$

Here, the N-electron system is taken to be the lowest neutral state. The value A of the electron affinity is negative if an anion is not stable with respect to the corresponding N-electron state, as for molecular wires with $n_r = 1, 1'$. (See Table I and Fig. 1.)

However, in a reassessment of Eq. (2), Sabin et al. [7] argued that it should be corrected to read

$$C_S = 1/(I - |A|). \tag{5}$$

That is, they asserted that the neutral-state capacitance should be independent of the sign of A and the stability of the lowest $(N + 1)$-electron anionic system.

TABLE I: Comparison of Molecular Capacitance Results. Quantum capacitances C_I and C_S of polyphenylene molecular wires, as determined from detailed DFT calculations, are reported as a function of the molecules' lengths and compared with scaled capacitances from three quasi-classical models. C_I and C_S were evaluated in units of fundamental positive charges per volt ($+e$/V) via Eqs. (2) and (5) in the text, based upon the detailed DFT calculations by the authors. With $+e$/V as the unit for capacitance and Angstroms for length, the permittivity of free space is $\epsilon_0 = 5.526349 \times 10^{-3}$ $+e$/V-Å. Values of C_S are omitted for $n_r \geq 2$, because $A > 0$ and $C_S = C_I$ in those cases. The scaling factors κ are set for the quasi-classical calculations in columns 11 to 13 to force them to match the value of C_I for $n_r = 12$.

No. Rings[a], n_r	Ellips-oid Geom.	Length, L (Å)	Approximate Mean Semiaxes of HOMO (Å) a	b	$c = \langle h \rangle$	I (eV)	A (eV)	C_I ($+e$/V)	C_S ($+e$/V)	$\kappa=0.963$ $4\pi\kappa\epsilon_0(abc)^{\frac{1}{3}}$ ($+e$/V)	$\kappa=0.654$ $4\pi\kappa\epsilon_0(ab^2)^{\frac{1}{3}}$ ($+e$/V)	$\kappa=0.335$ Eqs. (6) ($+e$/V)
1	oblate	4.97	2.319	2.131	0.4997	9.19794	−1.50122	0.0935	0.1299	0.093[b]	0.102[c]	0.039
1'	prolate	7.61	3.647	2.134	0.5851	8.55674	−0.52193	0.1101	0.1245	0.111	0.116	0.061
2	prolate	11.87	5.770	2.134	0.6705	7.53935	0.17230	0.1357		0.135	0.135	0.076
3	prolate	18.77	9.219	2.133	0.6698	6.96467	0.88079	0.1644		0.158	0.158	0.097
4	prolate	25.67	12.668	2.133	0.6691	6.66747	1.26095	0.1850		0.176	0.175	0.118
5	prolate	32.57	16.120	2.133	0.6689	6.48157	1.50209	0.2008		0.190	0.190	0.137
6	prolate	39.46	19.565	2.133	0.6686	6.34086	1.67425	0.2143		0.203	0.203	0.156
7	prolate	46.36	23.014	2.133	0.6685	6.25273	1.78319	0.2237		0.214	0.214	0.174
8	prolate	53.26	26.462	2.133	0.6685	6.17859	1.87711	0.2325		0.224	0.224	0.191
9	prolate	60.15	29.910	2.133	0.6684	6.11564	1.95121	0.2401		0.234	0.234	0.209
10	prolate	67.05	33.360	2.133	0.6684	6.06637	2.01368	0.2467		0.242	0.242	0.225
11	prolate	73.95	36.807	2.133	0.6683	6.02178	2.06447	0.2527		0.250	0.250	0.242
12	prolate	80.85	40.257	2.133	0.6683	5.98638	2.10945	0.2579		0.258	0.258	0.258

[a]One ring structure designated 1' is ethynyl-benzene. See Fig. 1.

[b]In column 11, formula used for $n_r = 1$ is $4\pi\kappa\epsilon_0(a^2c)^{\frac{1}{3}}$.

[c]In column 12, formula used for $n_r = 1$ is $4\pi\kappa\epsilon_0(a^2b)^{\frac{1}{3}}$.

Eqs. (2) and (5) each differ by a factor of $1/e^2$ from the ones actually written by Iafrate *et al.* and by Sabin *et al.* This unit transformation assumes that EAs and IPs are expressed in eV, as is common in tabulations [8] of molecular electron detachment energies. Then, Eqs. (2) and (5) yield capacitances in units of fundamental positive charges per volt, symbolized here as "$+e$/V".

Making no *a priori* judgment on the relative merits of Eqs. (2) and (5), we calculated the quantum capacitances of all the molecular wires using both formulas. The results for C_I and C_S are presented, respectively, in columns 9 and 10 of Table I. Of course, C_I and C_S are identical, except where $A < 0$—i.e., for $n_r = 1, 1'$. Thus, for $n_r \geq 2$ we omit the C_S values and points from column 10 of the table and from Fig. 2. The results from quasi-classical models for C_I and C_S appear in columns 11 and 12 of the table, respectively.

To obtain the capacitance results in Table I, for each of the molecular wires with ring numbers $n_r = 1$ through 12, we used the Gaussian 98 (and later the Gaussian 03) quantum chemistry program [9] to perform separate, detailed DFT calculations to determine the total energies $E(N-1)$, $E(N)$, and $E(N+1)$ of the respective charge states of interest—cation, neutral, and anion. For single-ring structures, we determined these three total energies for both benzene (C_6H_6), which we designate as $n_r = 1$, and the benzene ethynylene molecule ($C_6H_5-C\equiv C-H$), which we designate by $n_r = 1'$.

For each value of n_r, the calculations included a geometry optimization as part of the determination of the lowest-energy neutral state, but then that same neutral-state geometry was used in determining the lowest-energy states for the corresponding cation and anion. From the energies of these three states we determined the vertical IPs and EAs, in accordance with Eqs. (3) and (4), in order to evaluate Eq. (2) and Eq. (5) for the thirteen molecules $n_r = 1, 1', 2, \ldots, 12$. These capacitance results are presented in Table I and plotted versus molecular length L in Fig. 2 and versus r_{eq} in Fig. 3.

Because of the difficulty of calculating accurate EAs for organic molecules, especially for the longer molecular wires, it was necessary to use a large basis set and an accurate density functional method in performing the total energy calculations. Following the work of Schaefer and his collaborators [10, 11], as well as guidance from colleagues [12, 13] on the best means for evaluating EAs of organic molecules, we employed a large STO 6-31+G* Gaussian basis and the accurate B3LYP density functional. The geometry of the nuclear framework for each neutral state was optimized in this basis set.

To avoid any computational artifacts in the results, we also checked our computations by repeating them several times. We used alternate density functionals (B3PW91), basis sets (STO 6-31-G*), and software implementations (the MacSpartan program [14]). However, these calculations all produced essentially the same molecular geometries and also the same capacitance results within 3 or 4 per cent. We report in Table I and Fig. 2 results from the B3LYP/6-31+G* DFT calculations, since these can be repeated using both of the most commonly available

commercial software tools, Gaussian and MacSpartan.

While the values of I and A from the DFT calculations might not be as accurate for the longer OPE molecules, from assessments of DFT electron detachment energies [10, 11] the results here should be reasonably accurate for at least the shorter molecules we consider— e.g., the one- to four-ring (n_r=1-4) systems. Also, the I's and A's determined here for these shorter molecules are in good agreement with earlier published results [8], where they are available. Thus, we have confidence in the logarithmic and other trends reported in this paper, since they already are evident in our results from molecules with only n_r=1-4, and results we calculated for the longer molecules maintain those trends.

The molecular length L is the distance between the terminal H atoms on an OPE molecule's nuclear framework. By contrast, the semiaxis parameters a, b, and c in Table I approximate the mean dimensions of the molecule by estimating the dimensions of its highest occupied molecular orbital. In this, we follow the reasoning of Froese, who used the mean radius of the highest occupied atomic orbital to represent the radius of an atom [15]. We take the mean contour of the OPE HOMO to enclose an approximately ellipsoidal region of space extending above and below the plane of the molecule. Then, as a simple estimator of the length, $2a$, and the width, $2b$, of the π-type HOMO ellipsoid in a plane above and parallel to that of the molecular wire, we use, respectively, the length of its C-atom framework plus two Froese C-atom radii ($r_C = 0.92$ Å) and the width of the C-atom framework plus two C-atom radii. Dimensions of the C-atom frameworks were determined by DFT geometry optimizations, as part of our calculations of the molecular IPs and EAs.

For each of the molecules we also determined a mean half-thickness $c = \langle h \rangle$, where $\langle h \rangle = \int_0^\infty z|\phi_a(x,y,z)|^2 dz / \int_0^\infty |\phi_a(x,y,z)|^2 dz$ is the mean height of the π-type DFT HOMO ϕ_a at the middle of the molecule in the positive z-direction perpendicular to the molecular plane. This quantum calculation was performed for all the molecules with n_r even, then those values of $\langle h \rangle$ were interpolated for n_r odd and $n_r = 1'$. For benzene (n_r=1), though, $\langle h \rangle$ was determined above the position of a C atom, because the numerator and denominator of the expression for $\langle h \rangle$ vanish above the center of the molecular plane. Using these values of c provides a somewhat better 3-axis ellipsoid model for the shapes of these molecules, as determined by the shapes of their HOMOs. These are seen in orbital contour plots to have the approximate overall shapes of flattened ellipsoids, thicker in the middle and thinner toward the ends and edges.

III.   ANALYSIS

Analysis of the results presented in Fig. 2 and Table I shows that they may be explained or rationalized in terms of the isoperimetric model outlined in the introduction

to this paper. However, none of the many other quasi-classical models we tried succeeded in doing so. This is primarily because the L dependence of C_I for the molecular wires is fit by a logarithm to a high degree of confidence ($R^2 = 0.9975$), as are the identical values of C_S for $n_r \geq 2$. This unusual logarithmic length scaling of the capacitance does not conform to any of the usual models from classical electrostatics [6, 16] or from prior investigations of the quantum capacitance [7].

One might expect, for example, purely linear length scaling of the capacitance, as is exhibited by macroscopic cylindrical wires [6] or by macroscopic wires of any constant cross section. Alternatively, one might expect the molecular wire capacitances to scale much like those for classical ellipsoids of revolution [7, 17–19]:

$$C_{oblate} = 4\pi\epsilon_0\kappa\frac{\sqrt{a^2 - b^2}}{\sin^{-1}\left(\sqrt{a^2 - b^2}/a\right)}, \quad n_r = 1 \qquad (6a)$$

$$C_{prolate} = 4\pi\epsilon_0\kappa\frac{\sqrt{a^2 - b^2}}{\ln\left[\left(a + \sqrt{a^2 - b^2}\right)/b\right]}, \quad n_r \geq 1'. \quad (6b)$$

However, if the capacitances for a sequence of molecular wires were to scale simply like those of classical oblate and prolate ellipsoids with the approximate dimensions of the molecules, the capacitances would exhibit a quasi-linear dependence upon L. This is shown by using the values of a and b given in columns 4 and 5 of Table I to evaluate Eqs. (6) in column 13 of the table. These results all are scaled by $\kappa = 0.335$ to make $C_{prolate} = C_I$ for $n_r = 12$ and are plotted versus L as the +'s in Fig. 2. Plainly, their nearly linear behavior in L does not match, even qualitatively, the pronounced nonlinear behavior of the quantum results (black diamonds and ×'s). Similar comments apply to results from the classical formulas for capacitors of a number of other likely shapes (e.g., three-axis ellipsoid, truncated cylinder, chains of ellipsoidal disks). These also scale nearly linearly in L and, thus, are unsuccessful in fitting the quantum capacitances calculated for the OPEs via DFT.

Instead, after many diverse efforts to account for the OPE's logarithmic scaling behavior of C_I with L, we discovered from detailed exploration of the theory of isoperimetric inequalities [2] that Eq. (1) provides a close empirical match. In isoperimetric theory, Eq. (1) with C_0=0, or $4\pi\epsilon_0 r_{eq}$, gives the classical capacitance of a sphere with the same volume as is enclosed by a non-spherical conductor, and that capacitance provides a lower bound to the classical capacitance of the non-spherical conductor [2]. Here, $4\pi\epsilon_0 r_{eq}$ provides a lower bound for the classical capacitance of an ellipsoidal capacitor with approximate mean semiaxial dimensions of the OPE HOMO.

The reason the scaling behavior for this lower bound is exhibited by the molecule, instead of the behavior of an ellipsoidal capacitor, could be that the nodal structure of the π-type HOMO reduces the effective "surface area" on which positive charge can be distributed on each

neutral molecule. Thus, the capacitance of each would be less than might be expected from its otherwise ellipsoidal valence negative charge distribution.

While this rationale is not certain, it is certain that the lower bound $4\pi\epsilon_0 r_{eq}$ accounts remarkably well for the logarithmic scaling behavior with L exhibited by the quantum capacitances of the OPE molecules. This is seen in Fig. 2 and in the values of $4\pi\epsilon_0 r_{eq}$ in column 11 of Table I. The values from column 11 are plotted versus L as the open squares in Fig. 2. These values all incorporate the single empirically adjustable scaling factor $\kappa = 0.963$, which is set to ensure agreement with the C_I value in column 9 in just the $n_r = 12$ case. However, then all the points from this 3-axis quasi-classical model are in strikingly close correspondence with the quantum-derived C_I points (black diamonds), obtained using Eq. (2). Also, the logarithmic fit (dashed line) to the quasi-classical points is very strong ($\mathrm{R}^2 = 0.9909$) and in remarkable agreement with the logarithmic fit (solid line) to the values of C_I. Further, the value $\kappa = 0.963$ derived from this *ad hoc* use of $4\pi\epsilon_0 r_{eq}$ to fit the logarithmic scaling in L agrees well with the value $\kappa = \text{slope}/4\pi\epsilon_0 = 0.97$ determined from the slope of the regression line in Fig. 3, which formally fits C_I to r_{eq}.

The high degree of agreement of the logarithmic fits depicted in Fig. 2, plus the strong linear fit of C_I to r_{eq} shown in Fig. 3, justify the statements surrounding Eq. (1) at the outset of this paper. Also, they permit us to write $C_I \approx 4\pi\epsilon_0 \kappa (abc)^{\frac{1}{3}} + C_0$, where $C_0 = 0.0022$ $+e/\text{V}$. Then, elimination of C_I between this approximate relation and Eq. (2) yields, after minor rearrangement:

$$A \approx I - \frac{1}{4\pi\epsilon_0\kappa(abc)^{\frac{1}{3}} + C_0}. \qquad (7)$$

This equation provides a mutual constraint upon the ionization potentials, the electron affinities, and the mean dimensions of the HOMO of a non-spherical, neutral OPE molecular wire. It is the analog of a similar constraint that recently was demonstrated [1] for neutral atoms. As in the case of the atoms, Eq. (7) shows that positive values of the electron affinities A for the molecules become smaller as the dimensions of their highest occupied orbitals or their dielectric constants become smaller. Sometimes, as for the $n_r = 1, 1'$ cases here, the HOMO dimensions become so small that A is negative.

Taking $C_0 \approx 0$, we also evaluated Eq. (1) using only a 2-degree-of-freedom ellipsoid of revolution model, wherein we apply the constraints $c = a$ for $n_r = 1$, but $c = b$ for $n_r \geq 1'$. This produces the values in column 12 of Table I. Plotted as the open circles in Fig. 2, these quasi-classical points also are in striking agreement with the quantum results for $n_r \geq 2$. However, they yield slightly too high a capacitance estimate for the two single-ring systems, esp. the oblate benzene molecule ($n_r = 1$). This is because, as seen in the first two rows of columns 5 and 6 of the table, the b parameter in the ellipsoid of revolution model overestimates the thickness of these two shorter molecules; it

fails to follow the flattening that is measured more accurately in the 3-axis model by $c = \langle h \rangle$. Extending this reasoning to interpret the even higher values produced by C_S in these cases, one might say that, in effect, Eq. (5) overestimates the dimensions of the molecules even more.

As might be expected from Eq. (7), the flattening of the HOMOs for the neutral states of the two shortest molecular wires also corresponds to the values of their EAs—i.e, their A values—becoming negative. For this reason, when Eq. (5) discards the sign of A, the analysis above suggests that it simultaneously discards geometric information that is retained in the 3-axis model of the molecule and in Eq. (2). In effect, C_S attributes to benzene a positive value of A that could be sustained only by a molecule that is estimated to be much thicker or longer than is reasonable and consistent with dimensional estimates made for the still longer, prolate molecules. Thus, regardless of which of the formulas, Eqs. (2) or (5), represents a quantum capacitance more rigorously, the former, Iafrate *et al.* formula appears to exhibit greater sensitivity to the geometry of the neutral system. Also, values calculated with that formula increase monotonically with the system's length, which is an intuitively satisfying behavior for a capacitance.

Finally, we show that the observed logarithmic form of the scaling of the molecular wire capacitances with L can be explained or rationalized in terms of their linear scaling with r_{eq}. From Table I, we observe that for most of the OPE molecules $a \approx \frac{1}{2}L$, while b and c are nearly constant. Thus, we may write $r_{eq} = (abc)^{\frac{1}{3}} \approx (bc/2)^{\frac{1}{3}}(L)^{\frac{1}{3}}$. That is, since the values of C_I scale with r_{eq}, as noted above and seen in Fig. 3, they also must scale approximately with $L^{\frac{1}{3}}$. Alternatively, because b and c are nearly constant, we might view the capacitances for these molecular wires as scaling approximately as the cube root of a dimensionless length scaling parameter $\lambda = L/[2(bc)^{\frac{1}{2}}]$. Using this parameter, the inverse relationship between the exponential function and the natural logarithm permits the capacitance to be expanded in a Taylor series in powers of $\ln(\lambda)$:

$$C_I \approx C_0 + 4\pi\epsilon_0\kappa(bc)^{\frac{1}{2}}(\lambda)^{\frac{1}{3}} \qquad (8a)$$

$$\approx C_0 + 4\pi\epsilon_0\kappa(bc)^{\frac{1}{2}}\exp\left[\frac{1}{3}\ln(\lambda)\right] \qquad (8b)$$

$$\approx C_0 + 4\pi\epsilon_0\kappa(bc)^{\frac{1}{2}}\left[1 + \frac{1}{3}\ln(\lambda)\right. \qquad (8c)$$

$$\left. + \frac{1}{18}\ln^2(\lambda) + \frac{1}{162}\ln^3(\lambda) + \cdots\right].$$

In first order, the expansion Eq. (8c) establishes the essential logarithmic dependence of C_I on $L = 2(bc)^{\frac{1}{2}}\lambda$ that is seen in Fig. 2. Also, via numerical evaluation of the expansion, we have found that terms beyond the purely logarithmic first order expansion account for only 33 per cent of the total, infinite order value of the expansion for the longest of the molecular wires considered here. For the four shortest molecules, terms beyond first order account for less than 15 per cent of the total values.

By third order, for all the OPE molecules ($n_r = 1-12$) the expansion has converged within 4 per cent of the total values from Eq. (8a). Further, through all orders, capacitance values from the expansion are fit very well ($R^2 \geq 0.994$) by a regression function linear in $\ln(L)$.

A particularly simple physical interpretation for the capacitance scaling follows from Eqs. (8) when they are specialized to the ellipsoid of revolution model. Therein, we take $c = b$ and $\kappa = 0.65$, so that Eq. (8c) becomes $C_I \approx C_0 + (4\pi\epsilon_0\kappa b)[1 + \frac{1}{3}\ln(\lambda) + \cdots]$. The factor $4\pi\epsilon_0\kappa b$ is recognized readily as the classical capacitance of a sphere whose radius b is the half-width for a molecular wire (i.e., the half-width for a benzene ring). This factor does not vary appreciably as the wires get longer. Thus, physically, the other, non-linear factor $(\lambda)^{\frac{1}{3}} \approx 1 + \frac{1}{3}\ln(\lambda) + \cdots$ modulates the capacitance of that approximately benzene-sized spherical kernel to describe the scaling of C_I as the molecular wires and their valence electron distributions get longer and more prolate.

IV. SUMMARY AND CONCLUSIONS

It has been shown that a simple, quasi-classical capacitance formula, Eq. (1), accounts for diverse aspects of the scaling of the quantum capacitances of OPE molecular wires with their dimensions. The formula is based upon an isoperimetric [2] principle of classical electrostatics that does not appear to have been applied in quantum mechanics before. The isoperimetric formula fits both the logarithmic scaling of the molecules' quantum capacitances with their lengths and the linear scaling with their equivalent radii r_{eq}. Other capacitance formulas fail to do so.

Equation (1) generalizes to at least some non-spherical molecules the linear length scaling relation $C_I \approx C_{sphere} = 4\pi\epsilon_0\kappa\langle r\rangle_a + C_0$, which applies to spheres in classical electrostatics [6] and which has been observed [1] to govern the quantum capacitances of atoms. Equation (1) also helps reveal a previously unappreciated, simple relationship, Eq. (7), that connects the electron affinity, the ionization potential, and the dimensions of a molecular wire.

This reveals, too, the role of the scaling parameters and HOMO dimensions in determining a molecular wire's approximate "band gap," $(I-A)$, a quantity of importance in molecular electronics [20]. Similarly, Eq. (7) shows that the capacitance scaling parameters and the dimensions of the valence electron distribution can determine a molecule's chemical "hardness" [21], according to

$$\eta \equiv \frac{I-A}{2} \approx \frac{1}{2}\left(\frac{1}{4\pi\epsilon_0\kappa(abc)^{\frac{1}{3}}+C_0}\right). \quad (9a)$$

Thus, they also can have a role in determining its quantum chemical potential [22], according to

$$\mu \approx -\left(\frac{I+A}{2}\right) \approx -I + \frac{1}{2}\left(\frac{1}{4\pi\epsilon_0\kappa(abc)^{\frac{1}{3}}+C_0}\right). \quad (9b)$$

The chemical hardness, η, and chemical potential, μ, are quantities that are attributed much significance in density functional theories [23]. Relationships are established therein that describe the role of η and μ in governing a number of fundamental processes, such as the energy response to charge transfer [21, 23]. The hardness, in particular, has been applied to attempt to understand a range of chemical properties and behaviors [24]. Through those established relationships involving η and μ, plus Eqs. (9), the capacitance scaling parameters and HOMO dimensions might be used to determine and to interpret the characteristics of diverse phenomena.

Such insights would be based not just on the fact that the hardness is half the reciprocal of the charge capacitance [25] or quantum capacitance, $\eta = 1/2C_I$. They would rely upon the demonstration here that molecules, as well as atoms, appear to behave much like classical spherical capacitors.

If it can be shown to extend to other molecules, this principle, as embodied in Eqs. (1) and (7), also could be of considerable value in simplifying difficult, time-consuming calculations of molecular EAs. As for the molecular wires, the energetics of large molecules could be predicted from that of structurally similar, but smaller molecules. This might point, as well, toward a still more general electrostatics-like approach for determining the energetics of atoms and molecules in terms of their shapes and dimensions. Thus, capacitance scaling relations for other molecules and for atoms are to be explored further elsewhere.

[1] J. C. Ellenbogen, Phys. Rev. A **74**, 034501 (2006).

[2] G. Polya and G. Szegö, *Isoperimetric Inequalities in Mathematical Physics*, no. 27 in Annals of Mathematics Studies (Princeton Univ. Press, Princeton, NJ, 1951).

[3] G. J. Iafrate, K. Hess, J. B. Krieger, and M. Macucci, Phys. Rev. B **52**, 10737 (1995).

[4] J. Gazquez and E. Ortiz, J. Chem. Phys **81**, 2741 (1984).

[5] J. P. Perdew, Phys. Rev. B **37**, 6175 (1988).

[6] D. Halliday, R. Resnick, and J. Walker, *Fundamentals of Physics* (Wiley, New York, NY, 2001), sixth ed.

[7] J. R. Sabin, S. B. Trickey, S. P. Apell, and J. Oddershede, Int. J. Quantum Chem. **77**, 358 (2000).

[8] P. J. Lindstrom and W. G. Mallard, eds., *NIST Chemistry WebBook*, NIST Standard Reference Database No. 69 (Natl. Inst. of Standards and Technology, 2005), http://webbook.nist.gov/chemistry/.

[9] M. J. Frisch *et al.*, *Gaussian 98m (Revision a.11), Gaussian 98w (Revisions a.6 and a.7), and Gaussian 03 (Revision C.02)*, Gaussian, Inc., Wallingford, CT, 1998-2004.

[10] J. C. Rienstra-Kiracofe, C. J. Barden, S. T. Brown, and H. F. Schaefer III, J. Phys. Chem. A **105**, 524 (2001), and references cited therein.

[11] J. C. Rienstra-Kiracofe, C. J. Barden, S. T. Brown, and H. F. Schaefer III, Chem. Rev. **102**, 231 (2002).

[12] J. Seminario, private communications, 2001-02.

[13] W. T. Borden, private communications, 2001.

[14] *MacSpartan'02, Version 1.06*, Wavefunction, Inc., Irvine, CA, 1998-2004.

[15] C. Froese, J. Chem. Phys. **45**, 1417 (1966).

[16] G. Woan, *Cambridge Handbook of Physics Formulas* (Cambridge U. Press, Cambridge, UK, 2003).

[17] E. J. Garboczi, K. A. Snyder, J. F. Douglas, and M. F. Thorpe, Phys. Rev. E **52**, 819 (1995).

[18] A. Queiroz, *Capacitance Calculations* (2004), http://www.coe.ufrj.br/~acmq/tesla/capcalc.pdf.

[19] S. Das, unpublished derivation verifying Eqs. 6.

[20] M. A. Reed, Proc. IEEE **87**, 652 (1999).

[21] R. G. Parr and R. G. Pearson, J. Am. Chem. Soc. **105**, 7512 (1983).

[22] R. G. Parr, R. A. Donnelly, M. Levy, and W. E. Palke, J. Chem. Phys. **68**, 3801 (1978).

[23] W. Kohn, A. D. Becke, and R. G. Parr, J. Phys. Chem. **100**, 12974 (1996), and references cited therein.

[24] R. G. Pearson, ed., *Chemical Hardness* (Wiley-VCH, Weinheim, Germany, 1997), and references cited therein.
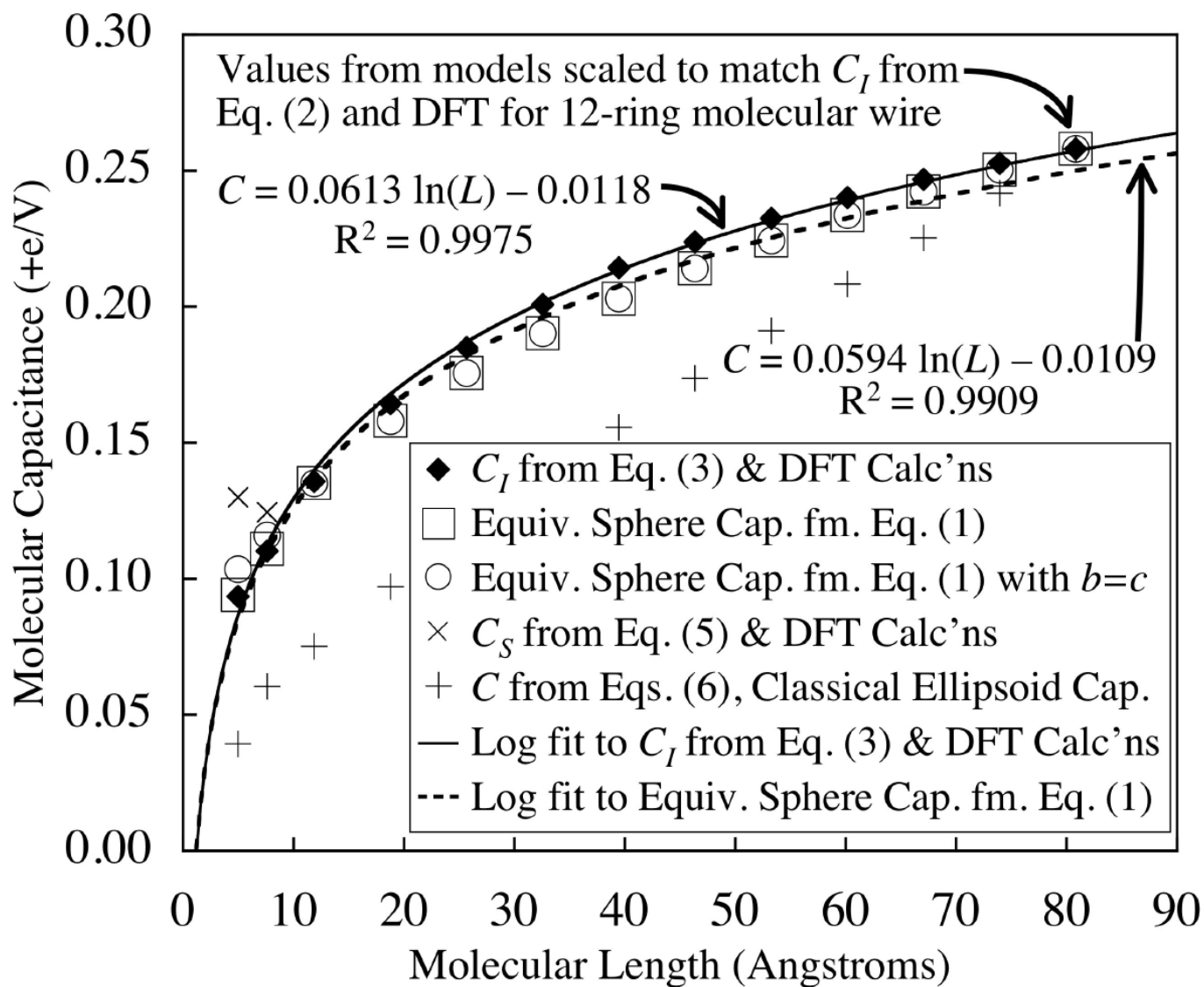
[25] P. Politzer, J. Chem. Phys. **86**, 1072 (1987).

Figure 2